

Cite this: *Chem. Commun.*, 2012, **48**, 1895–1897

www.rsc.org/chemcomm

## COMMUNICATION

## A highly sensitive fluorogenic chemodosimeter for rapid visual detection of phosgene†

Xuanjun Wu, Zhisheng Wu, Yuhui Yang and Shoufa Han\*

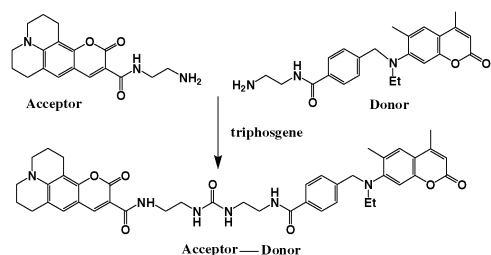
Received 28th November 2011, Accepted 12th December 2011

DOI: 10.1039/c2cc17411a

A highly sensitive chemodosimeter was identified from a panel of rhodamine derivatives for rapid and visual detection of phosgene with a detection limit of 50 nM triphosgene. Visual detection of gaseous phosgene with chemodosimeter absorbed paper strips was demonstrated.

Phosgene ( $\text{COCl}_2$ ) is a widely used chemical intermediate in industry to produce pesticides, isocyanate-based polymers, pharmaceuticals, *etc.*<sup>1</sup> Exposure to phosgene can cause severe damages to respiratory tracks and lungs, often leading to individual death.<sup>2</sup> As a colorless and highly toxic gas, phosgene had been used as a chemical warfare agent and is currently a potential agent for terrorist chemical attack. Hence methods allowing sensitive and rapid detection of phosgene are highly desirable to alert both the leakage of phosgene gas in industry and the purposeful deployment of phosgene.

Conventional assays for phosgene, *e.g.* gas chromatography, are often limited by poor portability or by the requirement of sophisticated procedures.<sup>3</sup> Optical sensors are advantageous as they use widely available instruments and offer the possibility of real-time visual detection of analytes. Several chemosensors,<sup>4,5</sup> *e.g.* analyte mediated aggregation of gold nanoparticles and chromogenic/fluorogenic reagents, have been developed to detect phosgene. One elegant strategy, as shown in Scheme 1,



**Scheme 1** A fluorescence resonance energy transfer (FRET) based method for detection of a phosgene simulant.<sup>4</sup>

Department of Chemical Biology, College of Chemistry and Chemical Engineering, and the Key Laboratory for Chemical Biology of Fujian Province Xiamen University, Xiamen, China 361005.

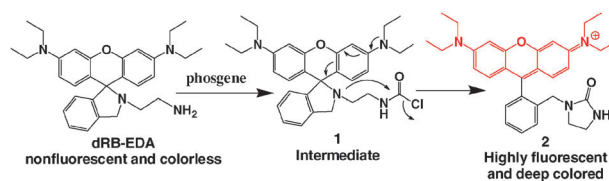
E-mail: shoufa@xmu.edu.cn; Tel: +86-0592-2181728

† Electronic supplementary information (ESI) available: Purification and characterization of compound **2**, fluorescence spectra of the colored species, assay procedures for triphosgene, and characterization of the reaction of triphosgene with rhodamine-hydroxamate, rhodamine-hydrazide and RB-EDA. See DOI: 10.1039/c2cc17411a

proceeded *via* triphosgene mediated hetero-dimerization of a fluorescent donor and an acceptor fluorophore.<sup>4</sup> The resultant proximity of the donor–acceptor pair imparts efficient intra-molecular fluorescence resonance energy transfer (FRET), leading to enhanced fluorescence emission of the acceptor upon excitation of the donor dye.<sup>4</sup> However, the formation of acceptor–acceptor or donor–donor homodimers could not be prevented under the assay conditions which compromised the assay efficiency. In addition, the detection limits of FRET based assays are often limited by interference due to overlap of emission of the donor with that of the acceptor.

Rhodamines are widely utilized in cellular imaging and biotechnology owing to their exceptional photophysical properties. Rhodamine-(deoxy)lactams, which are prone to analyte mediated opening of the spiro-(deoxy)lactam to give highly fluorescent and deep colored rhodamine fluorophores, have been extensively employed as the fluorogenic platforms for sensing of various metal ions and reactive chemicals.<sup>6</sup> Here we report the visual and chromo-fluorogenic detection of a phosgene simulant with *N*-(rhodamine B)-deoxylactam-ethylenediamine (referred as dRB-EDA) (Scheme 2), a highly sensitive chemodosimeter identified from a panel of rhodamine-(deoxy)lactams.

dRB-EDA, which was colorless and nonfluorescent, instantly turned into red color in dimethylformamide (DMF) upon addition of triphosgene. Triphosgene, the safer substituent of phosgene used in organic synthesis, decomposes into phosgene in the presence of tertiary amines in solution. Hence it was used as a phosgene simulant in previous research and in this report.<sup>4</sup> To optimize the assay conditions, the color formation rates of dRB-EDA with triphosgene in a variety of solvents containing triethylamine (TEA, 3%, v/v) were monitored by fluorescence emission. Fig. S1 (ESI†) shows that DMF was the preferred assay media compared to acetonitrile or aqueous DMF (ESI†). The assay was applicable in aqueous DMF containing 2% (v/v) of water, suggesting its compatibility



**Scheme 2** Low-background and chromo-fluorogenic detection of phosgene with nonfluorescent dRB-EDA.

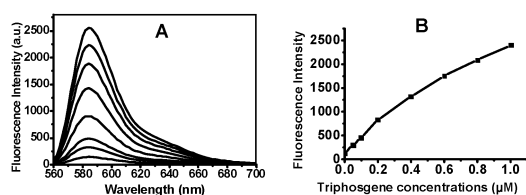


**Fig. 1** Fluorescence emission spectra of dRB-EDA (1 mg ml<sup>-1</sup>) in the presence of triphosgene (1, 0.8, 0.6, 0.4, 0.2, 0.1, 0.05 μM, from top to bottom) in DMF containing TEA (A). The titration curve was plotted by fluorescence emission intensity at 590 nm vs. analyte concentrations (B) ( $\lambda_{\text{ex}}$  @ 560 nm).

with practical applications where the moisture might be present in the samples. Kinetic analysis showed that the reaction between dRB-EDA and triphosgene completed immediately in various assay media (ESI<sup>†</sup>, Fig. S2) which were independent of the analyte concentrations.

To determine the detection limit, the fluorescence emission and UV-vis absorbance of dRB-EDA in DMF containing TEA were recorded vs. triphosgene concentration. Fig. 1 shows that the fluorescence emission intensity at 590 nm increased as a function of analyte concentration. As low as 50 nM of triphosgene was clearly identified under the assay conditions whereas a detection limit of 50 μM of triphosgene was reported for a FRET based system.<sup>4</sup> The new assay, with 3 orders of magnitude enhancement of sensitivity and low-background interference, is advantageous for practical applications where it is imperative to detect 0.1 or 2 ppm of gaseous phosgene (0.4–8 mg L<sup>-1</sup>), which are the thresholds for the low permissible exposure limit and the immediate danger to health and life limit.

The UV-vis absorption spectra of the reaction solutions revealed a new strong absorption band at 560 nm with dose dependent color intensities (Fig. 2). Compared with the colorless substrate, the deep colored species generated in the assay is highly visible, suggesting the potential utility of this assay for on-spot detection of phosgene with “naked eyes”.

With the detection limit established, we went on to determine the structures formed between triphosgene and dRB-EDA. Carbamoyl chlorides are readily generated upon nucleophilic substitution of phosgene with amines.<sup>7</sup> We reasoned that intermediate **1** should be formed when dRB-EDA reacts with triphosgene under alkaline conditions (Scheme 2). Since carbamoyl chlorides could be dehydrohalogenated *in situ* to give an isocyanate derivative,<sup>7</sup> intermediate **1** or its corresponding isocyanate species will undergo intramolecular cyclization to

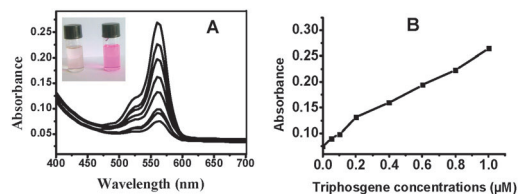


**Fig. 2** UV-vis absorption spectra of dRB-EDA (1 mg ml<sup>-1</sup>) in the presence of triphosgene (1, 0.8, 0.6, 0.4, 0.2, 0.1, 0.05 μM, from top to bottom) in DMF containing TEA (A), the inset shows the visual images of dRB-EDA with (left) or without (right) addition of triphosgene (1 μM); (B) the titration curve was plotted by absorbance at 560 nm vs. analyte concentration.

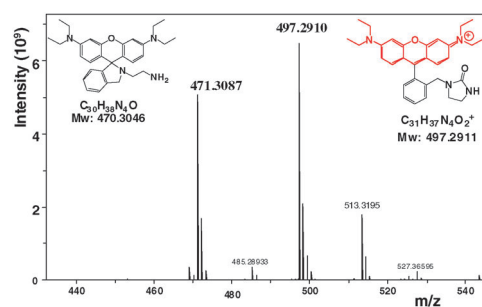


**Fig. 3** HRMS confirmation of the genesis of compound **2** in the reaction between dRB-EDA and triphosgene.

afford compound **2** as the colored species (Scheme 2; ESI<sup>†</sup>, Scheme S2). To probe the underlying mechanism of the chromogenic response of dRB-EDA towards triphosgene, the colored species generated in the assay solution was isolated by silica gel chromatography. High resolution mass spectrometry (HRMS) of the colored species revealed a major peak located at 497.2910 (Fig. 3), which was consistent with the theoretical molecular weight of compound **2** (497.2911). <sup>1</sup>H-NMR and <sup>13</sup>C-NMR spectra analysis (ESI<sup>†</sup>, Fig. S10 and S11) further supported the formation of compound **2** in the assay system. The fluorescence spectra of the assay solution were almost identical to those of rhodamine B (ESI<sup>†</sup>, Fig. S3 and S4). Taken together, the experimental data suggest the triphosgene triggered opening of the intramolecular deoxylactam of dRB-EDA under the assay conditions (Scheme 2).

We then explored the possible coupling of intermediate **1** with dRB-EDA in our assay (ESI<sup>†</sup>, Scheme S1). HRMS analysis of the assay solution containing excess dRB-EDA and triphosgene revealed the presence of compound **2** together with dRB-EDA whereas no dimers of dRB-EDA were detected (ESI<sup>†</sup>, Fig. S12). Since carbamoyl chlorides readily react with primary amines to afford ureas,<sup>7</sup> the absence of dimeric dRB-EDA (ESI<sup>†</sup>, Scheme S1) indicated that intramolecular rearrangement of intermediate **1** to compound **2** was highly rapid, which prevented the intermolecular coupling of intermediate **1** with dRB-EDA.

To explore the role of the deoxylactam of dRB-EDA in the chromogenic response for triphosgene, *N*-(rhodamine B)-lactam-ethylenediamine (referred as RB-EDA) was tested for its efficacy to detect triphosgene. RB-EDA differs from dRB-EDA in that it contains an amide moiety (Fig. 4A). Visual and spectroscopic analysis showed that no colored species was produced in the assay solution of RB-EDA with triphosgene (Fig. 4B), implying that the non-nucleophilic nature of the lactam impedes the intramolecular cyclization of RB-EDA (ESI<sup>†</sup>, Scheme S2). The differential responses of dRB-EDA and RB-EDA highlighted the crucial role of the deoxylactam of dRB-EDA in chromo-fluorogenic sensing of triphosgene.

Rhodamine-hydroxamate and rhodamine-hydrazide were evaluated next for their capability to sense triphosgene (Fig. 4A). Detection of triphosgene was achieved with a limit of 2 μM for rhodamine-hydroxamate and 20 μM for rhodamine-hydrazide (ESI<sup>†</sup>, Fig. S8–S11). HRMS analysis indicated that sensing of triphosgene with rhodamine-hydroxamate proceeded *via* a Lossen rearrangement based mechanism (ESI<sup>†</sup>, Scheme S3 and Fig. S13),

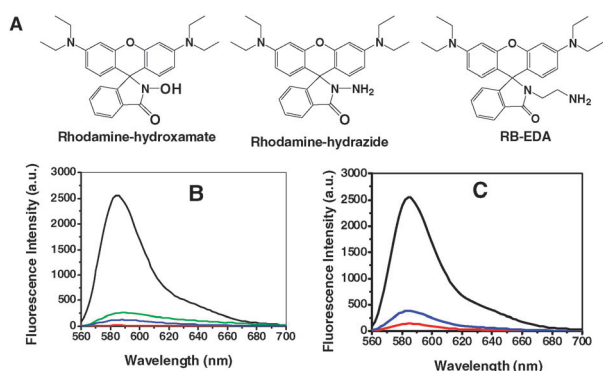


**Fig. 4** Assay efficiency of selected rhodamine-(deoxy)lactams. (A) Chemical structures of the rhodamine-(deoxy)lactam based chemodosimeters; (B) fluorogenic responses of rhodamine-hydroxamate (in green), rhodamine-hydrazide (in blue) and RB-EDA (in red) towards triphosgene (1  $\mu\text{M}$ ) in DMF as compared to dRB-EDA (in black); (C) fluorescence emission spectra of dRB-EDA (red) in DMF upon addition of triphosgene (1  $\mu\text{M}$ , in black) or formaldehyde (10 mM, in blue) ( $\lambda_{\text{ex}}$  @ 560 nm).

which is analogous to the reported sensing of diethyl chlorophosphate.<sup>8</sup> Consistent with the documentation that hydrazide could react with phosgene to form 1,3,4-oxadiazole,<sup>7</sup> HRMS indicated that the detection of triphosgene with rhodamine-hydrazide was achieved *via* phosphorylation triggered opening of the lactam, leading to a 1,3,4-oxadiazole containing rhodamine derivative (ESI<sup>†</sup>, Scheme S4 and Fig. S14). Albeit being able to detect triphosgene with rapid kinetics (ESI<sup>†</sup>, Fig. S3 and S4), rhodamine-hydroxamate and rhodamine-hydrazide were much inferior to dRB-EDA in terms of assay sensitivity.

A potential competitive reaction using dRB-EDA is the fluorogenic reaction with aldehydes.<sup>6c</sup> Fig. 4C shows that dRB-EDA could detect 1  $\mu\text{M}$  of triphosgene with superior sensitivity and assay kinetics relative to 10 mM of formaldehyde under the same assay conditions,<sup>6c</sup> suggesting its good selectivity in sensing of gaseous phosgene.

With the favorable features of dRB-EDA, we further probed its feasibility for real-time detection of gaseous phosgene in a portable manner. dRB-EDA was absorbed on paper strips and silica gel respectively. The testing paper was placed in sealed chambers where gaseous phosgene was generated *in situ* from triphosgene and phenanthridine following a reported procedure.<sup>9</sup> The test paper quickly turned into red color upon generation of gaseous phosgene whereas no color was observed in the control chambers (Fig. 5). The color change of the strips was clearly visible in the presence of 0.8  $\text{mg L}^{-1}$  of gaseous phosgene, which is 10-fold more sensitive than the threshold of immediate danger to health and life limit of gaseous phosgene (ESI<sup>†</sup>, Fig. S17). In a separate experiment, the colorless silica gel column containing dRB-EDA quickly became red in contact with gaseous phosgene (ESI<sup>†</sup>, Fig. S18 and S19). These results indicated that visual detection of gaseous phosgene is applicable with dRB-EDA formulated with appropriate portable platforms, *e.g.* paper strips.

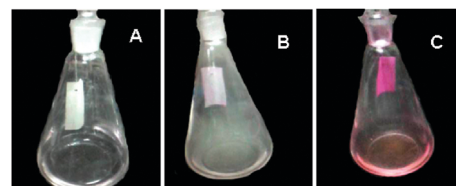


**Fig. 5** Visual detection of gaseous phosgene with dRB-EDA absorbed paper strips. The strips were placed in sealed flasks containing phenanthridine (A), triphosgene (B) or phenanthridine and triphosgene (C) and then immediately photographed.

In summary, dRB-EDA, a rhodamine-deoxylactam containing chemodosimeter, was demonstrated to be sensitive for sensing of triphosgene with a detection limit of 50 nM. The assay proceeds *via* analyte triggered opening of the deoxylactam of dRB-EDA and afforded deep-colored and highly fluorescent species. Given the promptness of the color formation, low-background interference, and high sensitivity of this assay, dRB-EDA is attractive for on-spot detection of gaseous phosgene with routine instruments or “naked eyes”.

This work was supported by grants from NSFC (No. 21072162 and 20802060), Natural Science Foundation of Fujian Province of China (No. 2011J06004), the Fundamental Research Funds for the Central Universities (No. 2011121020) and NEFTBS (No. J1030415).

## Notes and references

- (a) *Br. Med. J.*, 1939, **2**, 1243; (b) J. J. Collins, D. M. Molenaar, L. O. Bowler, T. J. Harbourt, M. Carson, B. Avashia, T. Calhoun, C. Vitano, P. Ameis, R. Chalfant and P. Howard, *J. Occup. Environ. Med.*, 2011, **53**, 239.
- (a) W. I. Glass, *N. Z. Med. J.*, 1972, **75**, 121; (b) S. A. Cucinell, *Arch. Environ. Health*, 1974, **28**, 272.
- (a) G. G. Esposito, D. Lillian, G. E. Podolak and R. M. Tuggle, *Anal. Chem.*, 1977, **49**, 1774; (b) H. H. Hill Jr. and S. J. Martin, *Pure Appl. Chem.*, 2002, **74**, 2281; (c) R. Jeltos, E. Burghardt and J. Breman, *Br. J. Ind. Med.*, 1971, **28**, 96–99; (d) M. H. Noweir and E. A. Pfitzer, *Am. Ind. Hyg. Assoc. J.*, 1971, **32**, 163; (e) L. J. Priestley, Jr., F. E. Critchfield, N. H. Ketcham and J. D. Cavender, *Anal. Chem.*, 1965, **37**, 70; (f) H. B. Singh, D. Lillian and A. Appleby, *Anal. Chem.*, 1975, **47**, 860; (g) C. R. Thompson, G. H. Farrah, L. V. Haff, A. W. Hook, J. S. Jacobson, E. J. Schneider and L. H. Weinstein, *Health Lab. Sci.*, 1976, **13**, 71.
- H. Zhang and D. M. Rudkevich, *Chem. Commun.*, 2007, 1238.
- (a) S. K. Dangwal, *Ind. Health*, 1994, **32**, 41; (b) D. Feng, Y. Zhang, W. Shi, X. Li and H. Ma, *Chem. Commun.*, 2010, **46**, 9203; (c) S. Virj, R. Kojima, J. D. Fowler, J. G. Villanueva, R. B. Kaner and B. H. Weiller, *Nano Res.*, 2009, **2**, 135.
- (a) Q. A. Best, R. Xu, M. E. McCarroll, L. Wang and D. J. Dyer, *Org. Lett.*, 2010, **12**, 3219; (b) H. N. Kim, M. H. Lee, H. J. Kim, J. S. Kim and J. Yoon, *Chem. Soc. Rev.*, 2008, **37**, 1465; (c) Z. Li, Z. Xue, Z. Wu, J. Han and S. Han, *Org. Biomol. Chem.*, 2011, **9**, 7652; (d) X. Wu, Z. Wu and S. Han, *Chem. Commun.*, 2011, **47**, 11276.
- H. Babad and A. G. Zeiler, *Chem. Rev.*, 1973, **73**, 75–91.
- S. Han, Z. Xue, Z. Wang and T. B. Wen, *Chem. Commun.*, 2010, **46**, 8413–8415.
- H. Eckert and J. Auerweck, *Org. Process Res. Dev.*, 2010, **14**, 1501.